Chem

CellPress
OPEN ACCESS

Article

Probing enantioinduction in confined chiral spaces through asymmetric oxime reductions

Elizabeth D. Heafner,[1,2] Andrew L. Smith,[1,3] Cristina V. Craescu,[1,2,3] Kenneth N. Raymond,[1,2] Robert G. Bergman,[1,2] and F. Dean Toste[1,2,4,*]

[1]Department of Chemistry, University of California at Berkeley, Berkeley, CA 94720, USA
[2]Chemical Sciences Division, Lawrence Berkeley National Laboratory, Berkeley, CA 94720, USA
[3]These authors contributed equally
[4]Lead contact
*Correspondence: fdtoste@berkeley.edu
https://doi.org/10.1016/j.chempr.2024.11.006

THE BIGGER PICTURE The ubiquity of chiral elements in natural products, pharmaceuticals, and fine chemicals has led to significant advancements in catalyst design and mechanistic understanding of asymmetric catalyst scaffolds. Enantiopure supramolecular hosts present a manmade catalytic scaffold with the ability to leverage a suite of non-covalent and electrostatic interactions, much like enzymes. Developing an understanding of the mechanism and interactions through which these systems impart selectivity is critical to their rational employment but has been the focus of little study. Herein, we utilize reaction scope and mechanistic investigation with data-science-based analysis to interrogate features of host-guest and substrate-substrate interactions involved in the asymmetric reduction of aryl, heteroaryl, and aliphatic oximes. The experimental and computational framework described herein provides guidelines to inform future studies on enantioinduction in supramolecular hosts.

SUMMARY

Enzyme-like enantiopure supramolecular hosts leverage non-covalent and electrostatic interactions to engage substrates in a chiral environment without direct coordination. Elucidating the mechanistic underpinnings of enantioinduction in these systems is critical to the success of this nascent field. We report herein an enantiopure $Ga_4L_6^{12-}$ host-catalyzed asymmetric reduction of aromatic, heteroaromatic, and aliphatic oximes to hydroxylamines, without N–O bond cleavage, using pyridine borane as a reductant cofactor. The reaction scope and mechanistic study, in combination with data science analysis, showcase that guest recognition and enantioinduction are highly sensitive to both steric and electronic effects. Optimization of interactions between the host, oxime, and reductant within the host cavity enabled highly enantioselective reactivity (>99% ee) for even previously unreported pyridine oximes. The emergent principles outlined herein lay the foundation for future applications of these promising catalytic scaffolds toward challenging synthetic targets.

INTRODUCTION

The development of a mechanistic understanding of enantioinduction is critical in asymmetric catalysis for the development of next-generation catalysts and methods. Among the most selective catalysts, enzymes have evolved to achieve exquisite selectivity through the synergistic action of an array of highly substrate-specific non-covalent and electrostatic interactions within a confined active site. Despite advancements in directed evolution and protein engineering, the widespread adoption of enzymes in asymmetric catalysis is still hampered by the limited range of reactions for which known enzyme counterparts can serve as a starting point for evolution campaigns.[1] On the other hand, chiral small-molecule catalysts are generally much more substrate promiscuous and can catalyze a wide range of asymmetric reactions. While their synthetic modularity enables a high degree of tunability, achieving enzyme-like selectivity is inherently challenging since these catalysts generally rely on a limited range of interactions accessible at specific sites on the catalyst to confer selectivity.[2–4] The application of supramolecular chemistry toward asymmetric catalysis exploits the ability of host molecules to stabilize reactive intermediates and conformations within a sterically confined cavity through a variety of non-covalent and electrostatic interactions.[5,6]

Please cite this article in press as: Heafner et al., Probing enantioinduction in confined chiral spaces through asymmetric oxime reductions, Chem (2024), https://doi.org/10.1016/j.chempr.2024.11.006

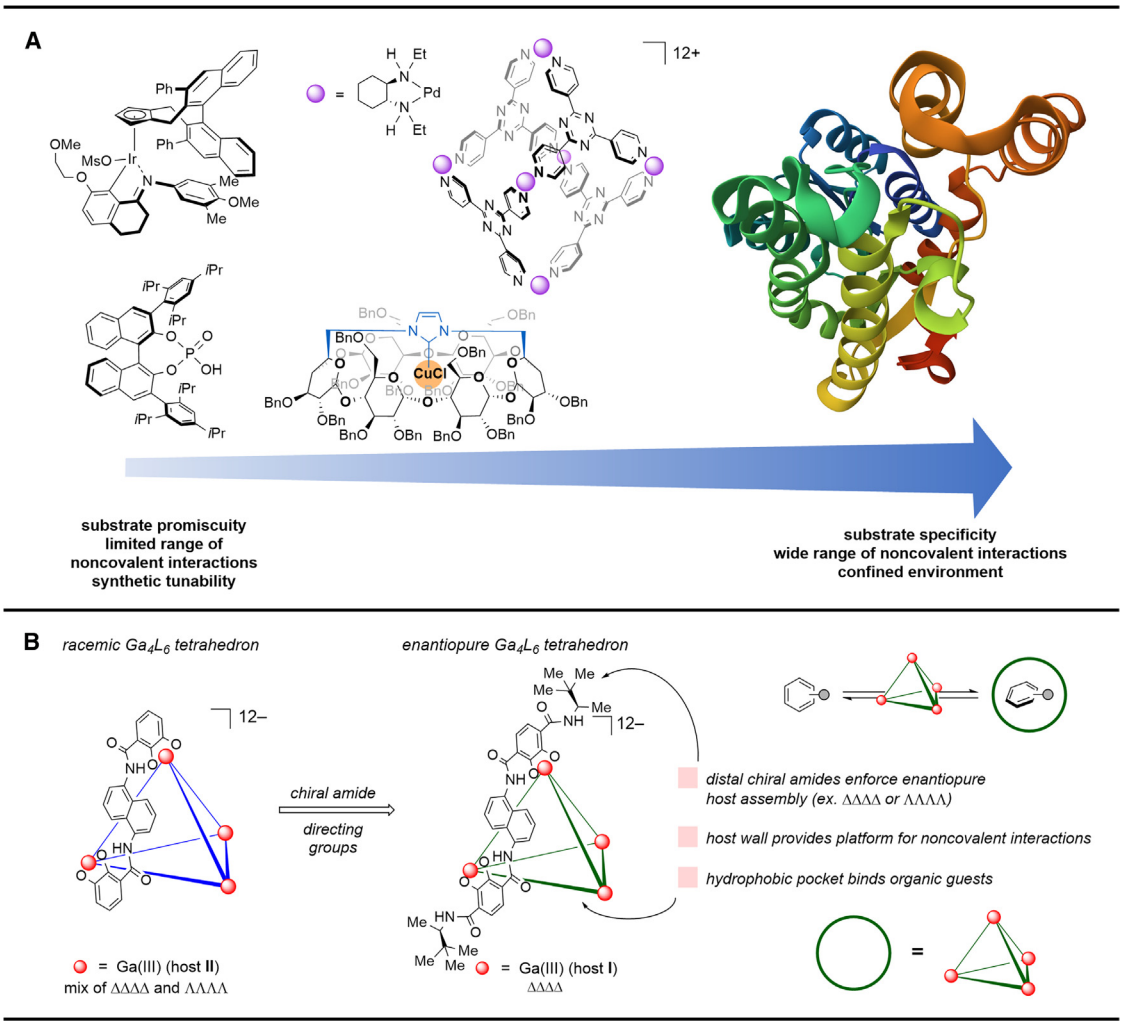

Figure 1. Features of asymmetric supramolecular catalysts

(A) Supramolecular hosts utilize features of chiral small-molecule catalysts and enzymes.

(B) Characteristics of racemic and enantiopure supramolecular $Ga_4L_6^{12-}$ tetrahedra used here and relevant to catalysis.

Supramolecular hosts therefore have the potential to complement traditional asymmetric catalyst platforms by leveraging the advantageous features of both enzymatic and chiral small-molecule catalyst systems to engage a broad range of substrates in a non-covalent interaction-rich synthetic microenvironment (Figure 1A).

Further understanding and structural diversification of supramolecular assemblies have resulted in a range of chemo- and regioselective reactions, yet asymmetric supramolecular catalysis is still largely underexplored and poorly understood. The few existing reports often describe the ability of host molecules to affect reactivity and selectivity when known chiral small-molecule catalysts are incorporated within the host scaffold[7–14] or encapsulated within a racemic or achiral host.[15,16] However, these approaches still rely heavily on the mode of activation utilized by the small-molecule catalyst, often through covalent bonding. In addition, the former approach results in host structures tailored to the reaction of interest and therefore may not be applied more generally. In contrast, enantiopure hosts lacking chiral small-molecule catalysts present an alternative catalytic scaffold with a distinct mode of enantioinduction—reactivity and selectivity are driven solely through non-covalent host-guest interactions within the cavity. The host scaffold therefore is not specific to a reaction or substrate type and can utilize an ensemble of non-covalent and electrostatic interactions with substrates on a case-by-case basis to achieve selectivity for a range of reactions. Examples of catalysis among enantiopure hosts are exceedingly few, and existing work has thus far focused on the development of new hosts to try to modulate enantioselectivity in well-understood model reactions.[17–22] Given that little is known of the interactions or substrate features important for enantioinduction within these hosts, the development and optimization of highly selective reactions utilizing enantiopure supramolecular hosts remain exceedingly difficult. For example, while host recognition of guest size and shape is understood to be important for guest encapsulation,[6,23–27] its

Please cite this article in press as: Heafner et al., Probing enantioinduction in confined chiral spaces through asymmetric oxime reductions, Chem (2024), https://doi.org/10.1016/j.chempr.2024.11.006

impact on enantioselectivity has been assumed rather than demonstrated. Interrogation of the interactions between host and substrate through the systematic study of reaction scope and mechanism is therefore a critical step in the elaboration of asymmetric supramolecular catalysis. However, current reports lack the broad substrate scopes necessary to adequately study enantioinduction in these systems.

The enantiopure Raymond $Ga_4L_6^{12-}$ tetrahedron, a commonly utilized catalytically active enantiopure host, was identified as a scaffold of particular interest for study (Figure 1B). Although not well understood itself, it maintains many of the properties of the well-studied parent racemic $Ga_4L_6^{12-}$ host. Its bis-catecholamide-based ligands are structurally analogous to those of the racemic host but also feature distal chiral amides proximal to the metal centers, which reinforce host enantiopurity as a result of strong mechanical coupling and thereby prevent catalyst racemization events (Figure 1B).[18,28] The dodecanionic charge of the host enables its solubility in polar solvents such as water, while the cavity of the host remains hydrophobic, enabling preferential encapsulation and stabilization of hydrophobic and cationic species.[25,29,30] These properties position the host to promote numerous acid-catalyzed reactions, including those proceeding through iminium-type intermediates. A previous study using the racemic $Ga_4L_6^{12-}$ host toward reductive amination also reported the preparation of a small number of racemic aliphatic hydroxylamines from oximes,[31] a class of compounds featuring an electron-rich C=N bond and labile N–O bond. Enantioselective oxime reductions to hydroxylamines have garnered interest in recent years because of the reduction's difficulty; the relatively low reactivity of oxime C=N bonds requires forcing reduction conditions that often additionally result in N–O bond cleavage.[32–38] To date, only three examples of enantioselective oxime reductions to aryl hydroxylamines have been reported to use Ir-based[39,40] and Ni-based[41] catalysts.

Such a synthetic challenge presents an interesting opportunity to study the capabilities of enantiopure supramolecular hosts as catalytic scaffolds. Given the precedent for racemic-host-catalyzed oxime reductions, we envisioned that reductions of a broad range of oximes in the enantiopure $Ga_4L_6^{12-}$ host might help elucidate key interactions involved in enantioinduction, particularly when paired with data science. Data-science-based analysis is particularly advantageous over traditional transition-state modeling in these systems because of the highly complex and therefore computationally demanding nature of supramolecular hosts.

RESULTS AND DISCUSSION

Developing the scope of enantioselective host-catalyzed oxime reductions

On the basis of precedent for aryl oxime reductions using transition-metal catalysts and aliphatic oxime reductions using the racemic $Ga_4L_6^{12-}$ host, initial work investigated the asymmetric reduction of acetophenone oxime (**2a**) and 2-pentanone oxime (**2b**) using pyridine borane (**1a**) as a reductant within enantiopure $Ga_4L_6^{12-}$ host **I** under air. After optimization (see Table S1 for **2a** and Table S2 for **2b**), **I** afforded the desired (*S*)-1-phenylethylhydroxylamine (**3a**) from **2a** in 97% ee and (*S*)-*N*-(pentan-2-yl)hydroxylamine (**3b**) from **2b** in 51% ee (Figure 2A for **2a** and Figure 2B for **2b**). Notably, no overreduction to the corresponding amine was detected. Control reactions with oxime **2a** and the chiral ligand precursor for host **I**, in the absence of host **I**, likewise afforded no product. Moreover, attempted reduction of oxime **2a** with a host whose cavity was blocked by strongly binding phosphonium salts showed no reaction in D_2O. However, low but detectable amounts of reactivity were observed with blocked host **I** in D_2O alone using oxime **2b**, which was eliminated under buffered D_2O conditions at pD 7.7 (see supplemental methods section "control experiments" for experimental details). These experiments are most consistent with the requirement for encapsulation within the host cavity for catalysis. Thus, reactivity occurs within the host cavity rather than on the host exterior. Comparable reactivity and enantioselectivity to the opposite enantiomer were observed when the $\Lambda\Lambda\Lambda\Lambda$, rather than $\Delta\Delta\Delta\Delta$, host was used with **2a** (see Table S1). Although enantioselectivity was achieved, the two oximes were reduced in disparate selectivity, which we hypothesized could be due to differing interactions accessible to each substrate during the enantiodetermining step.

We then considered a wide array of 53 small, synthesizable oximes without bias to known or unknown capacity for asymmetric reduction to search for potential trends underlying reactivity and selectivity (see Figure S7 for unsuccessful substrates). The catalytic activity of host **I** proved highly sensitive to substrate sterics when aryl oximes, obtained as (*E*):(*Z*) mixtures of isomers, were subjected to optimized reaction conditions (Figure 2C). Most notably, the use of oxime ethers (**2j**), rather than free oxime, as substrate decreased the yield and enantioselectivity markedly. Background control using **2j** and blocked **I** showed no reactivity, suggesting that the –OH group could be involved in important interactions with the host or pyridine borane. Although substrates featuring *ortho*-methyl (**2k**) and methoxy (**2l**) groups were reduced in high enantioselectivity, substrates with *ortho* halogens (**2m** and **2n**) displayed noticeably attenuated enantioselectivity compared with that of **2a**. *Meta* substituents (**2o**–**2s**) were generally well tolerated in that all afforded excellent enantioselectivity (92%–99% ee) except bromo-containing oxime **2s**, which was reduced in good selectivity (75% ee). Notably, oxime **2q**, which features a basic nitrogen, was well tolerated. Although very limited substitution was tolerated at the *para* position, 4-fluoro acetophenone oxime (**2t**) displayed sluggish reactivity but high enantioselectivity, which was further improved by the addition of a *meta* substitutent (**2u**). A competition experiment between **2a** and **2t** using 1 equiv of pyridine borane found consumption solely of **2a**, while **2t** was fully recovered, ruling out host decomposition mediated by **2t** (see supplemental methods section "competition experiment with oximes **2a** and **2t**" for details). Oximes featuring longer aliphatic side chains were generally very reactive; those with both linear (**2v**) and branched (**2w**) acyclic chains displayed moderate enantioselectivity. Bicyclic indanone (**2x**) likewise displayed moderate selectivity, whereas tetralone (**2y**) oximes displayed very poor enantioselectivity. Although substrate shape clearly appeared to affect enantioselectivity, no clear intuitive stereoelectronic trends emerge upon inspection.

Additional aliphatic oximes were also explored, and it was found that linear aliphatic oximes lacking any clear steric or

Please cite this article in press as: Heafner et al., Probing enantioinduction in confined chiral spaces through asymmetric oxime reductions, Chem (2024), https://doi.org/10.1016/j.chempr.2024.11.006

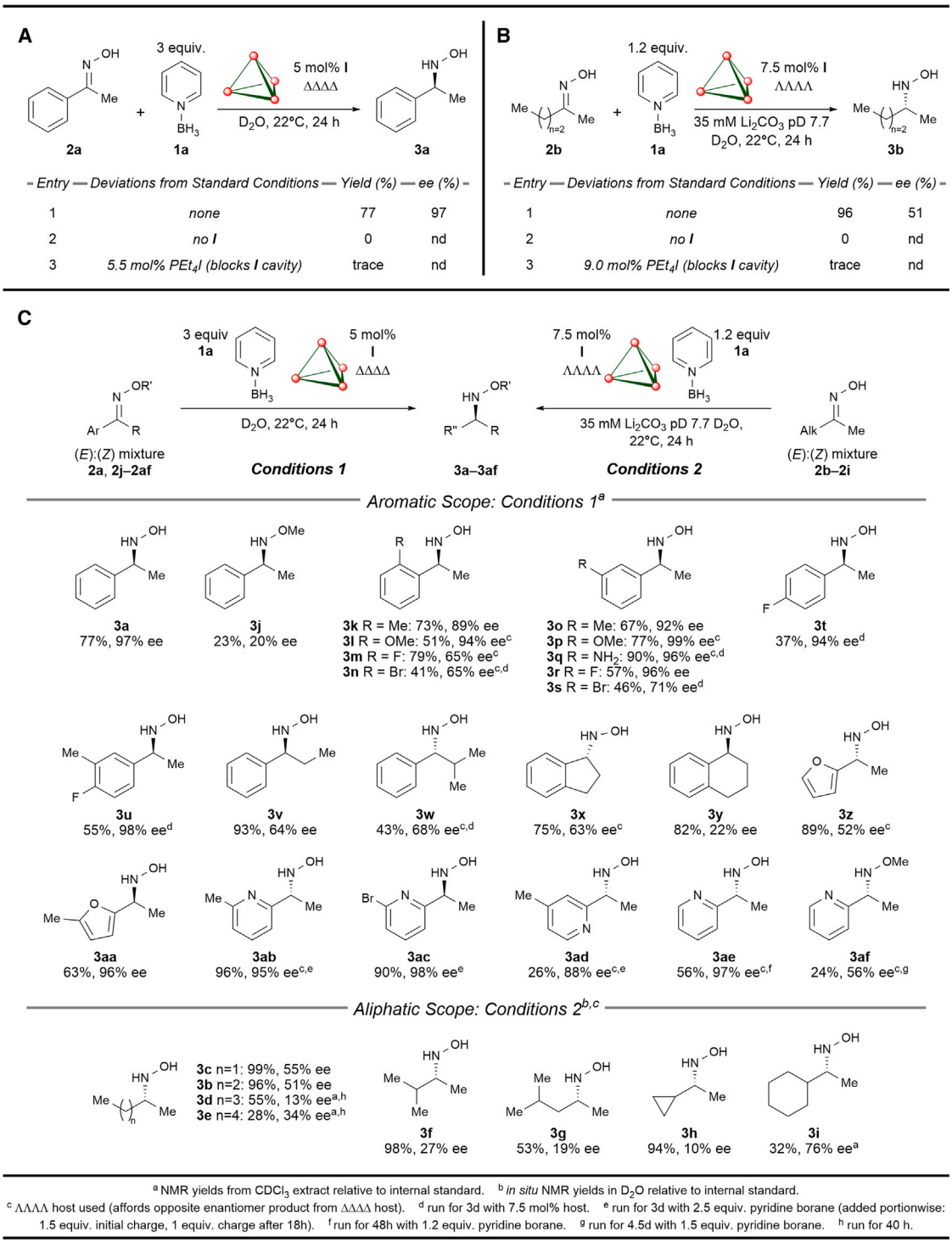

[a] NMR yields from $CDCl_3$ extract relative to internal standard. [b] *in situ* NMR yields in D_2O relative to internal standard.
[c] ΛΛΛΛ host used (affords opposite enantiomer product from ΔΔΔΔ host). [d] run for 3d with 7.5 mol% host. [e] run for 3d with 2.5 equiv. pyridine borane (added portionwise: 1.5 equiv. initial charge, 1 equiv. charge after 18h). [f] run for 48h with 1.2 equiv. pyridine borane. [g] run for 4.5d with 1.5 equiv. pyridine borane. [h] run for 40 h.

Figure 2. Reaction controls and scope

(A and B) Preliminary investigation of the asymmetric reduction of aryl oxime **2a** (A) and aliphatic oxime **2b** (B).

(C) Oximes successfully reduced using pyridine borane (**1a**) plus enantiopure host **l** system.

Please cite this article in press as: Heafner et al., Probing enantioinduction in confined chiral spaces through asymmetric oxime reductions, Chem (2024), https://doi.org/10.1016/j.chempr.2024.11.006

electronic biases (**2c**–**2e**) were generally reduced in higher yields and enantioselectivities than their more sterically bulky branched (**2f** and **2g**) or cyclic (**2h**) counterparts (Figure 2C). In fact, 2-butanone oxime **2c** (55% ee) was the most selective among the linear oximes investigated. As the length of the alkyl chain in the oxime increased (**2b**, **2d**, and **2e**), the observed reactivity and enantioselectivity diminished, suggesting that smaller oximes are better able to capture favorable interactions within the host cavity. However, cyclohexyl-containing oxime **2i** was a notable exception to this trend in that it produced the desired hydroxylamine in a reasonable 76% ee. Such a clear break in the selectivity trend suggests unique host-guest interactions for this substrate relative to other aliphatic oximes.

Given the ability of **I** and **1a** to successfully reduce oxime **2q** with excellent enantioselectivity, heterocyclic oximes were also of interest. Because the host metal lacked an open coordination site, we hypothesized that various heterocyclic oximes, including those featuring a basic, coordinating nitrogen, might also reasonably be tolerated under host-catalyzed reaction conditions. Furan **2z** was found to yield hydroxylamine in modest enantioselectivity, which was greatly improved with a pseudo-*meta* methyl group (**2aa**). Very limited examples of racemic reduction of pyridine-based oximes have been reported,[42,43] and we have found no reports of their enantioselective reduction. We note that pyridine-containing heterocyclic oximes, such as **2ab**, were not reduced under conventional pyridine borane reduction conditions in the absence of host. In the presence of racemic host II, however, oxime **2ab** was successfully reduced to the corresponding hydroxylamine nearly quantitatively (see supplemental methods section "general procedure H for the racemic synthesis of N-heterocyclic hydroxylamines" and hydroxylamine **3ab**" for more details). When subjected to enantiopure host **I** under optimized conditions, the oxime was reduced to the desired hydroxylamine (**3ab**) in near quantitative yield with excellent enantioselectivity. Subjecting oximes **2ac** and **2ae** to the host-**I**-catalyzed reaction yielded similar results, and 4-substituted oxime **2ad** yielded dramatically diminished reactivity with slightly diminished selectivity. Surprisingly, methyl ether oxime **2af** was reduced with attenuated but modest selectivity compared with that of parent oxime **2ae**, in contrast to that observed with acetophenone-derived oximes (**2a** versus **2j**).

In light of the decreased enantioselectivity observed with some oximes, we probed background reactivity by examining the reactivity of substrates **2v**, **2x**, **2y**, and **2z** in the presence of host **I** and blocking agent tetraethylphosphonium iodide. Under these inhibited host conditions, only trace product was observed, thus eliminating the possibility of competing racemic background reactivity eroding enantioselectivity. The observed differences in both reactivity and enantioselectivity between even subtly different substrates therefore suggest that highly specific interactions with substrates inside the host cavity may be involved in enantioinduction. However, few trends clearly emerged from initial crude analysis of the entire dataset to suggest one or more interactions involved in enantioinduction across substrates. In general, aryl and heteroaryl oximes were reduced in higher selectivity than aliphatic oximes. That aryl oxime ethers and non-methyl ketone-derived oximes were poorly or moderately tolerated suggests that added bulk around the oxime could hinder selectivity. Additional ^{19}F-NMR titration experiments in D_2O are also generally consistent with this hypothesis. Reactive aryl oximes featuring a free –OH (**2m** and **2t**) displayed the formation of additional ^{19}F peaks upon the addition of an excess of pyridine borane, whereas an unreactive methyl ether oxime did not display additional peaks after as much as 3 equiv of pyridine borane was added (see supplemental methods section "^{19}F NMR titrations" for more details). All together, these findings suggest that oxime shape, particularly with respect to steric bulk around the oxime functionality, could indeed be important for enantioinduction in the host.

Profiling the reaction mechanism toward understanding enantioinduction

To gain a clearer mechanistic picture, we undertook a rigorous mechanistic investigation. A series of *in situ* ^{19}F-NMR kinetics experiments were conducted on substrate **2m** (see supplemental methods section "kinetics experiments" for full details) under homogeneous conditions. Variable time normalization analysis[44] demonstrated that the reaction proceeds with first order in the host. Varying equivalents of **1a** indicated that the reductant is at saturation above 1 equiv, and ^{1}H-NMR indicated that it undergoes rapid exchange with **I** on the NMR timescale (see supplemental methods section "representative ^{1}H NMR spectra of reactants and host"). Much like that of pyridine borane, the ^{1}H-NMR of oxime with **I** indicated rapid guest exchange on the NMR timescale in the absence of pyridine borane, suggesting that oxime does not bind strongly within the host (see supplemental methods section "representative ^{1}H NMR spectra of reactants and host"). The observed linearity of the logarithmic reaction profile in oxime beyond 50% conversion is therefore consistent with the first order in oxime and suggests a rate-limiting step involving host and oxime. We also conducted kinetic isotope effect (KIE) experiments[45] to more clearly define the rate-limiting step. A primary solvent KIE was observed when reductions were run in H_2O or D_2O (Figure 3B). Conversely, a weak primary KIE was observed with **2a** (Figure 3C) and **2z** (see supplemental methods section "kinetic isotope experiments") in one-pot intermolecular competition experiments using a 1:1 mixture of pyridine borane-H_3 and pyridine borane-D_3. No KIE on reaction rate was observed when pyridine borane-H_3 and pyridine borane-D_3 were independently measured in parallel with **2m** (Figure 3D), suggesting that pyridine borane is not involved in the rate-limiting step. Combined, these results imply rate-determining encapsulation of protonated oxime followed by irreversible hydride delivery to furnish the desired hydroxylamine (Figure 3A). The need for stoichiometric or superstoichiometric quantities of **1a** for optimal conversion (see Tables S1 and S2) suggests that pyridine borane delivers only one hydride before extrusion to regenerate the empty host (Figure 3A). The observed H_2 evolution throughout the reaction, as well as the recovery of pyridine at the end of the reaction, also supports this analysis.

Kinetic and thermodynamic analysis of the binding behavior in **I** of (*R*) and (*S*) cationic arenes (see supplemental methods section "selective inversion recovery (SIR) NMR experiments" for details), selected to resemble protonated oxime, provided insight into the enantiodetermining step, which was hypothesized

Please cite this article in press as: Heafner et al., Probing enantioinduction in confined chiral spaces through asymmetric oxime reductions, Chem (2024), https://doi.org/10.1016/j.chempr.2024.11.006

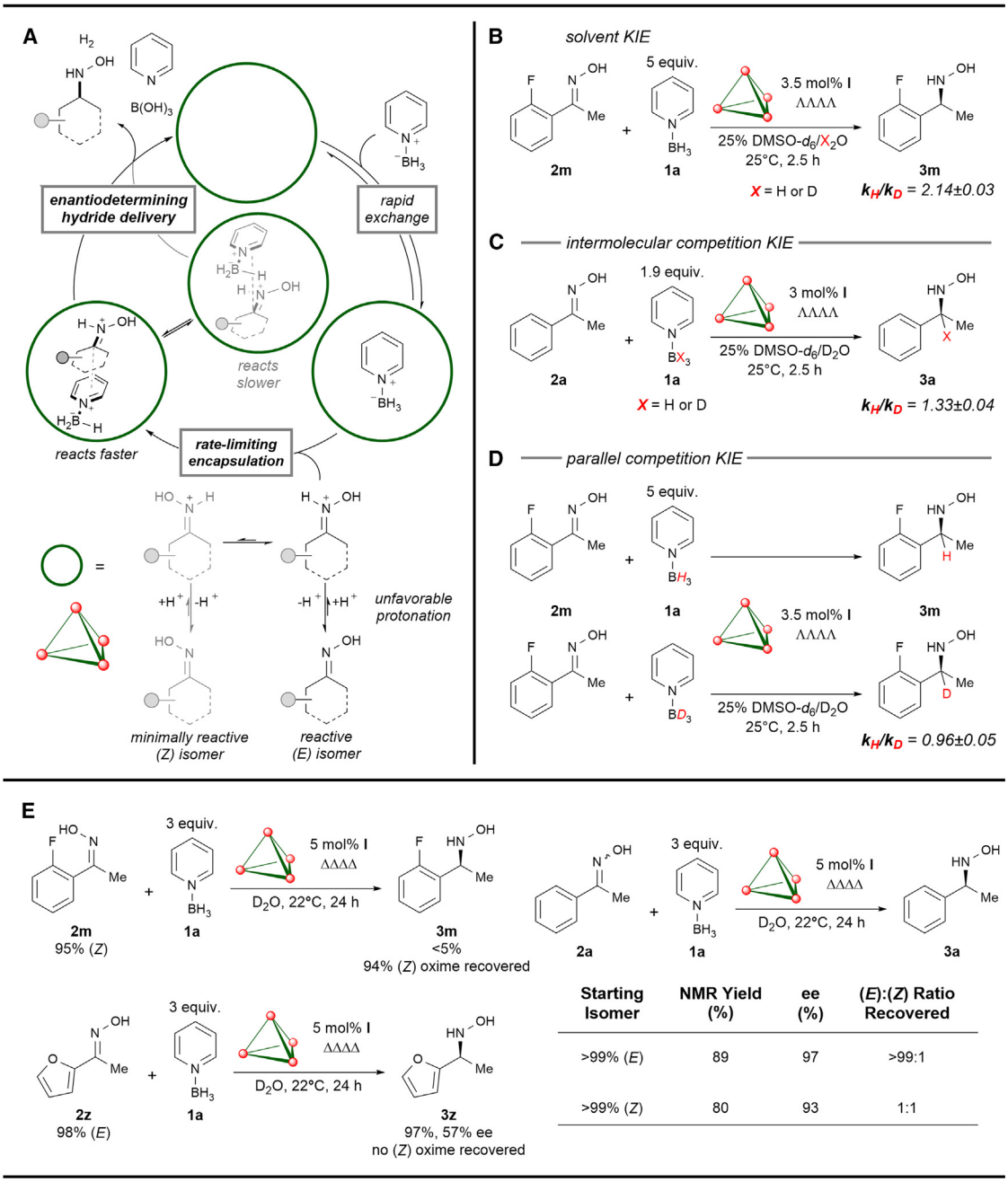

Starting Isomer	NMR Yield (%)	ee (%)	(E):(Z) Ratio Recovered
>99% (E)	89	97	>99:1
>99% (Z)	80	93	1:1

Figure 3. Mechanistic analysis of the host-catalyzed reduction

(A) Mechanistic analysis implicates rate-limiting encapsulation and enantiodetermining hydride delivery.

(B–D) Solvent KIE (B), intermolecular competition KIE of reductant (C), and parallel competition KIE of reductant (D). KIE values are reported as KIE ± standard deviation.

(E) Differing reactivity of oxime isomers under reaction conditions with enantiopure host **I**.

to be hydride delivery. Selective inversion recovery NMR analysis indicated that **I** displays only slight differences in guest exchange rates (only 1.3 times faster) between the two enantiomers, implying that encapsulation cannot be sufficiently selective to account for the observed enantioselectivities. Furthermore, a binding competition experiment between (*R*) and (*S*) arene with **I** indicated no preferential binding for one enantiomer over another, and the addition of an excess of **1a** did not perturb the equilibrium. Therefore, although the encapsulation event is kinetically rate limiting, enantioinduction is most likely achieved through Curtin-Hammett control of the transient, prochiral reductant-oxime complexes during hydride delivery (Figure 3A).

Please cite this article in press as: Heafner et al., Probing enantioinduction in confined chiral spaces through asymmetric oxime reductions, Chem (2024), https://doi.org/10.1016/j.chempr.2024.11.006

The observed enantioenrichment is therefore influenced by biased interactions, most likely an array of non-covalent interactions between the reductant, oxime, and host cavity wall, to preferentially stabilize one diastereomeric transition state over the other.

We hypothesized that concurrent reactivity of both the (*E*) and (*Z*) oxime isomers within the host could be the source of the lower enantioselectivities observed with some substrates. However, many of the least selective oximes (**2j**, **2x**, and **2y**) were isolated only as the (*E*) isomer. Furthermore, during the course of kinetic analysis, the (*E*) isomer of oxime **2m** was consumed, whereas the amount of (*Z*) oxime present remained constant. To probe this finding, we subjected enriched (*Z*) oxime **2m** to reaction conditions, which yielded less than 5% hydroxylamine and unreacted oxime (94% [*Z*]), consistent with the (*E*) isomer's being the only reactive species and indicating minimal to no isomerization (Figure 3E). However, when highly enriched (*Z*) oxime **2a** was similarly subjected to reaction conditions, hydroxylamine **3a** was formed in comparable yield and with high enantioselectivity to the same enantiomer as observed when an (*E*):(*Z*) mixture was used (Figures 2A and 3E). Furthermore, an approximately 1:1 (*E*):(*Z*) ratio of **2a** was recovered, suggesting that oxime isomerization can occur. Highly enriched (*E*) **2a** and **2z** also formed hydroxylamine in identical or highly comparable enantioselectivity as observed with the (*E*):(*Z*) mixture, and notably, no (*Z*) oxime was recovered, suggesting that only (*Z*)-to-(*E*) isomerization occurs during the reaction. Control experiments in the absence of pyridine borane suggested that this isomerization is host catalyzed rather than a result of background reactivity (see supplemental methods section "oxime isomerization control experiments" for details). Combined, these results suggest that host-catalyzed isomerization helps to funnel oxime mixtures to the much more reactive (*E*) isomer and that it is possible for comparatively much slower (*Z*) isomer to concurrently react with lower enantioselectivity. Oximes **2m** and **2w** appear to be exceptions to this regime given that very little to no isomerization was observed between oxime isomers. Therefore, the decreased enantioselectivity observed is most likely due to differential interactions within the host cavity between (*E*) oxime, reductant, and host rather than competing reactivity of oxime isomers.

Data science describes molecular features correlating to enantioinduction

With this mechanistic information and reaction scope, we turned to data-science-based analysis to help elucidate important reaction features. We used an in-house python workflow to parameterize reactive oximes into chemically meaningful descriptors (see supplemental methods section "general calculation workflows" for complete details). Although oxime isomer and protonation states were examined, parameterization of the protonated form of (*E*)-oximes provided the best correlation, and given the above data, these are the most mechanistically relevant species to the reaction outcome. No clear trend was observed between oxime size and reactivity, and in fact, many of the reactive oximes proved larger than unreactive oximes (see supplemental methods section "reactivity analysis" for more details), so attention was directed toward studying the features that might be involved in enantioinduction. We applied principal-component analysis (PCA) to condense the many-dimensional space into a more concise, holistic representation of the dataset. A *k*-means clustering algorithm on this chemical space indicated that the 30-oxime substrate scope considered could be represented by four distinct classes (Figure 4A). Across the entire dataset, a univariate correlation was observed with enantioselectivity using solely ground-state sterimol_L, a feature conveying molecular length (see supplemental methods section "oxime identity impacts performance of univariate correlation to observed enantioselectivity" for more details). Notably, analysis of the error associated with predictions of oximes belonging to separate clusters revealed that the largest deviations were primarily located in a single set of substrates. The addition of a second variable, namely ground-state buried volume at the oxime α-C (4 Å radius), generated an improved correlation (R^2 = 0.67) with the observed enantioselectivity across the entire dataset (Figure 4B; see supplemental methods section "unsupervised clustering reveals subset of oximes perform better with bivariate correlation" for more details). In analyzing the observed correlation, we noted that longer molecular length, as indicated by sterimol_L, and less hindered oximes, as indicated by the buried volume descriptor, each contribute to greater enantioinduction. Given that both variables generally describe steric properties, these findings provide data-based support for the hypothesis that guest size and shape are important for host-mediated enantioinduction.

Experimental and data science analysis of sterics and electronics effects on enantioselectivity

The identification of hydride delivery as the enantiodetermining step within the host cavity implies that tuning the reductant and host identities should affect enantioselectivity. Although non-covalent interactions with the host are often hypothesized as playing key roles in racemic and enantioselective catalysis in supramolecular hosts,[46–48] the interactions between substrates in multicomponent enantioselective reactions within supramolecular hosts have been the subject of little study. To probe for potential interactions between oxime and pyridine borane, we calculated interaction energies[49] between the oxime substrate and a pyridine probe molecule (see supplemental methods sections "non-covalent interactions" and "data science analysis of stereoelectronic effects on enantioselectivity" for full workflow details and calculations). Given that steric parameters correlated with enantioselectivity, we posited that they may also be important to the interaction between substrate and reductant. We noted that oxime ground-state sterimol_L also correlated with the interaction energy between pyridine and substrate (R^2 = 0.66). Importantly, this steric parameter captures the magnitude of a non-covalent interaction between reactants while also correlating to the enantioselectivity of their reaction.

To further qualify the nature of these non-covalent interactions, we tested pyridine boranes (**1a**–**1e**) with differing stereoelectronic profiles by using a selected subset of oximes (Figure 4; see supplemental methods section "pyridine borane reductant screens" for other oximes tested). Interaction energies of the Boltzmann distribution of conformations were calculated for each pyridine derivative with the protonated (*E*) isomer of the

Please cite this article in press as: Heafner et al., Probing enantioinduction in confined chiral spaces through asymmetric oxime reductions, Chem (2024), https://doi.org/10.1016/j.chempr.2024.11.006

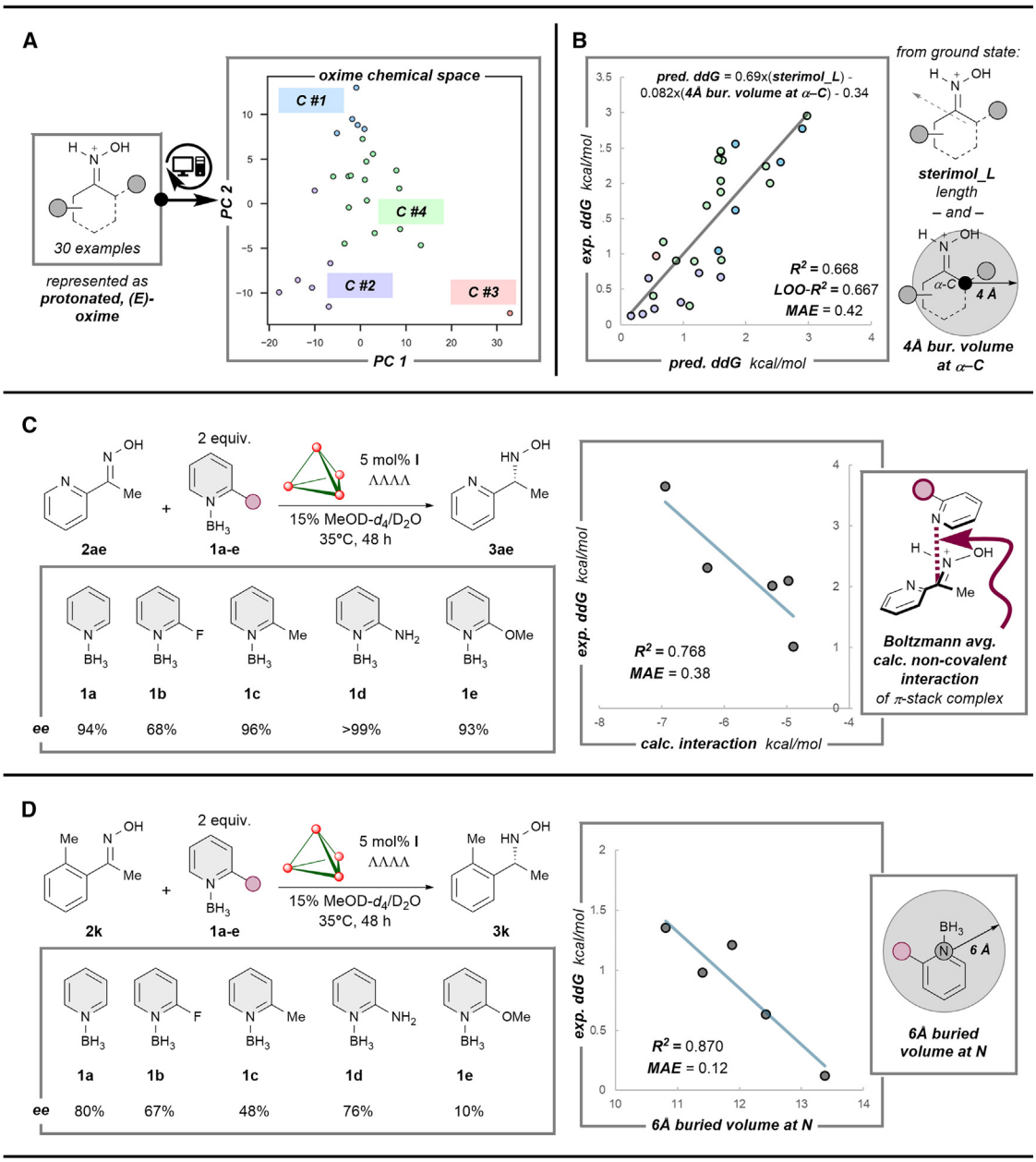

Figure 4. Interrogating interactions involved in enantioinduction through data science and Hammet-type analysis

(A) Oximes considered in linear regression tasks constitute four clusters (*k*-means clustering) across principal-component-reduced chemical space.

(B) Regression analysis shows the impact of oxime size and shape on interactions with the host for enantioinduction as represented by ground state sterimol_L and buried volume at the oxime α-C (4 Å).

(C) Reductant choice affects the enantioselectivity of pyridine oxime **2ae** reduction as a result of borane electronics according to correlation to calculated non-covalent interactions in the proposed enantiodetermining complex.

(D) Enantioselectivity of aryl oxime **2k** reduction displays dependence on borane sterics according to correlation to buried volume at the *N*-atom of the reductant.

corresponding oximes (see supplemental methods sections "analysis of correlations between non-covalent interactions calculated and enantioselectivity" and "analysis of correlations between pyridine borane features and enantioselectivity" for calculations). A positive correlation was observed between enantioselectivity and the interaction energies for pyridine-based oxime **2ae** (R^2 = 0.77; Figure 4C), suggesting that electronic effects dominate selectivity-determining interactions for this oxime. On the other hand, a negative correlation between the buried volume at the pyridine borane reductant and enantioselectivity was observed for **2k** (R^2 = 0.87; Figure 4D), suggesting that steric effects may be more important for the selectivity of

this oxime. Notably, these correlations do not exist across every oxime tested. Together, these correlations align with experimental observations highlighting the importance of both steric and electronic features for guest interactions within the host cavity and strongly suggest that interactions important for enantioselectivity are likely to vary on a substrate-to-substrate basis. The unexpected disparities observed between the relative importance of steric and electronic effects on the selectivity of individual substrates will be the subject of future investigation.

Conclusions

We report the application of an enantiopure $Ga_4L_6^{12-}$ supramolecular host for the asymmetric reduction of oximes to hydroxylamines under mild conditions. The host's unique structure and mode of enantioinduction enable the reduction of a broad range of aryl, aliphatic, and heteroaryl oximes, including the first examples of oximes featuring Lewis basic metal-coordinating functionalities, such as pyridine-based oximes. The substrate scope and mechanistic work, in combination with data science analysis, demonstrate the importance of guest size and shape in their interactions with the host for enantioselectivity. However, a solely steric-based model for enantioinduction in these systems paints an incomplete picture of host-guest interactions, as electronic effects are also demonstrated to be at play. Modulating the pyridine borane reductant cofactor reveals the importance of steric and electronic matching of guests on a substrate-by-substrate basis in multicomponent reactions to achieve high selectivity. The scope of this reaction, coupled with the mechanistic and statistical framework described herein, highlights the potential of supramolecular hosts in asymmetric catalysis and provides a foundation for further interrogation of enantioinduction in these systems.

METHODS

Details of general synthetic procedures, compound characterization (including NMR spectra and high-performance liquid chromatography [HPLC]) procedures for data science analysis, and coordinates for the density functional theory (DFT)-optimized structures can be found in the supplemental information.

RESOURCE AVAILABILITY

Lead contact

Requests for further information and resources should be directed to and will be fulfilled by the lead contact, F. Dean Toste (fdtoste@berkeley.edu).

Materials availability

All materials generated in this study are available from the lead contact without restriction.

Data and code availability

The data and code supporting the findings of this study are available in the manuscript, in the supplemental information, or from the lead contact without restriction.

ACKNOWLEDGMENTS

This research was supported by the Division of Chemical Sciences, Geosciences, and Bioscience within the Basic Energy Sciences Program of the US Department of Energy Office of Science at Lawrence Berkeley National Laboratory (DE-AC02-05CH1123). Computational and data science research was supported by the US National Science Foundation under the CCI Center for Computer-Assisted Synthesis (CHE-2202693). We thank the Pines Magnetic Resonance Center's Core NMR Facility (PMRC Core) for the resources provided and the staff, especially Dr. Hasan Celik, for their assistance. Instruments in CoC-NMR are supported in part by NIH S10OD024998.

AUTHOR CONTRIBUTIONS

Project conceptualization: E.D.H. and F.D.T.; resources, supervision, project administration, and funding acquisition: F.D.T.; experimental work: E.D.H. and C.V.C.; computational work: A.L.S.; writing: E.D.H. and F.D.T.; reviewing and editing: all authors.

DECLARATION OF INTERESTS

The authors declare no competing interests.

SUPPLEMENTAL INFORMATION

Supplemental information can be found online at https://doi.org/10.1016/j.chempr.2024.11.006.

Received: June 30, 2024
Revised: September 28, 2024
Accepted: November 13, 2024
Published: December 23, 2024

REFERENCES

1. Chen, K., and Arnold, F.H. (2020). Engineering new catalytic activities in enzymes. Nat. Catal. *3*, 203–213. https://doi.org/10.1038/s41929-019-0385-5.
2. Knowles, R.R., and Jacobsen, E.N. (2010). Attractive noncovalent interactions in asymmetric catalysis: links between enzymes and small molecule catalysts. Proc. Natl. Acad. Sci. USA *107*, 20678–20685. https://doi.org/10.1073/pnas.1006402107.
3. Neel, A.J., Hilton, M.J., Sigman, M.S., and Toste, F.D. (2017). Exploiting non-covalent π interactions for catalyst design. Nature *543*, 637–646. https://doi.org/10.1038/nature21701.
4. Proctor, R.S.J., Colgan, A.C., and Phipps, R.J. (2020). Exploiting attractive non-covalent interactions for the enantioselective catalysis of reactions involving radical intermediates. Nat. Chem. *12*, 990–1004. https://doi.org/10.1038/s41557-020-00561-6.
5. Morimoto, M., Bierschenk, S.M., Xia, K.T., Bergman, R.G., Raymond, K.N., and Toste, F.D. (2020). Advances in supramolecular host-mediated reactivity. Nat. Catal. *3*, 969–984. https://doi.org/10.1038/s41929-020-00528-3.
6. Piskorz, T.K., Martí-Centelles, V., Spicer, R.L., Duarte, F., and Lusby, P.J. (2023). Picking the lock of coordination cage catalysis. Chem. Sci. *14*, 11300–11331. https://doi.org/10.1039/D3SC02586A.
7. Hatano, M., Mizuno, T., Izumiseki, A., Usami, R., Asai, T., Akakura, M., and Ishihara, K. (2011). Enantioselective Diels-Alder reactions with anomalous endo/exo selectivities using conformationally flexible chiral supramolecular catalysts. Angew. Chem. Int. Ed. *50*, 12189–12192. https://doi.org/10.1002/anie.201106497.
8. García-Simón, C., Gramage-Doria, R., Raoufmoghaddam, S., Parella, T., Costas, M., Ribas, X., and Reek, J.N.H. (2015). Enantioselective hydroformylation by a Rh-catalyst entrapped in a supramolecular metallocage. J. Am. Chem. Soc. *137*, 2680–2687. https://doi.org/10.1021/ja512637k.
9. Guo, J., Xu, Y.-W., Li, K., Xiao, L.-M., Chen, S., Wu, K., Chen, X.-D., Fan, Y.-Z., Liu, J.-M., and Su, C.-Y. (2017). Regio- and enantioselective photodimerization within the confined space of a homochiral ruthenium/palladium heterometallic coordination cage. Angew. Chem. Int. Ed. *56*, 3852–3856. https://doi.org/10.1002/anie.201611875.

10. Ueda, Y., Ito, H., Fujita, D., and Fujita, M. (2017). Permeable self-assembled molecular containers for catalyst isolation enabling two-step cascade reactions. J. Am. Chem. Soc. *139*, 6090–6093. https://doi.org/10.1021/jacs.7b02745.

11. Tan, C., Jiao, J., Li, Z., Liu, Y., Han, X., and Cui, Y. (2018). Design and assembly of a chiral metallosalen-based octahedral coordination cage for supramolecular asymmetric catalysis. Angew. Chem. Int. Ed. *57*, 2085–2090. https://doi.org/10.1002/anie.201711310.

12. Hatano, M., Sakamoto, T., Mizuno, T., Goto, Y., and Ishihara, K. (2018). Chiral supramolecular u-shaped catalysts induce the multiselective Diels–Alder reaction of propargyl aldehyde. J. Am. Chem. Soc. *140*, 16253–16263. https://doi.org/10.1021/jacs.8b09974.

13. Xu, G., Leloux, S., Zhang, P., Meijide Suárez, J., Zhang, Y., Derat, E., Ménand, M., Bistri-Aslanoff, O., Roland, S., Leyssens, T., et al. (2020). Capturing the monomeric (L)CuH in NHC-capped cyclodextrin: cavity-controlled chemoselective hydrosilylation of α,β-unsaturated ketones. Angew. Chem. Int. Ed. *59*, 7591–7597. https://doi.org/10.1002/anie.202001733.

14. Ruan, J., Li, Z., Yin, C., Lu, Y.-L., Wei, Z.-W., Hu, P., and Su, C.-Y. (2024). Enantioselective [2+2] cross-photocycloaddition enabled by a chiral cage reactor via multilevel-selectivity control. ACS Catal. *14*, 7321–7331. https://doi.org/10.1021/acscatal.4c01087.

15. Bräuer, T.M., Zhang, Q., and Tiefenbacher, K. (2016). Iminium catalysis inside a self-assembled supramolecular capsule: modulation of enantiomeric excess. Angew. Chem. Int. Ed. *55*, 7698–7701. https://doi.org/10.1002/anie.201602382.

16. Bräuer, T.M., Zhang, Q., and Tiefenbacher, K. (2017). Iminium catalysis inside a self-assembled supramolecular capsule: scope and mechanistic studies. J. Am. Chem. Soc. *139*, 17500–17507. https://doi.org/10.1021/jacs.7b08976.

17. Nishioka, Y., Yamaguchi, T., Kawano, M., and Fujita, M. (2008). Asymmetric [2 + 2] olefin cross photoaddition in a self-assembled host with remote chiral auxiliaries. J. Am. Chem. Soc. *130*, 8160–8161. https://doi.org/10.1021/ja802818t.

18. Zhao, C., Sun, Q.-F., Hart-Cooper, W.M., DiPasquale, A.G., Toste, F.D., Bergman, R.G., and Raymond, K.N. (2013). Chiral amide directed assembly of a diastereo- and enantiopure supramolecular host and its application to enantioselective catalysis of neutral substrates. J. Am. Chem. Soc. *135*, 18802–18805. https://doi.org/10.1021/ja411631v.

19. Zhao, C., Toste, F.D., Raymond, K.N., and Bergman, R.G. (2014). Nucleophilic substitution catalyzed by a supramolecular cavity proceeds with retention of absolute stereochemistry. J. Am. Chem. Soc. *136*, 14409–14412. https://doi.org/10.1021/ja508799p.

20. Hart-Cooper, W.M., Zhao, C., Triano, R.M., Yaghoubi, P., Ozores, H.L., Burford, K.N., Toste, F.D., Bergman, R.G., and Raymond, K.N. (2015). The effect of host structure on the selectivity and mechanism of supramolecular catalysis of Prins cyclizations. Chem. Sci. *6*, 1383–1393. https://doi.org/10.1039/C4SC02735C.

21. Bierschenk, S.M., Pan, J.Y., Settineri, N.S., Warzok, U., Bergman, R.G., Raymond, K.N., and Toste, F.D. (2022). Impact of host flexibility on selectivity in a supramolecular host-catalyzed enantioselective aza-Darzens reaction. J. Am. Chem. Soc. *144*, 11425–11433. https://doi.org/10.1021/jacs.2c04182.

22. Sokolova, D., Piccini, G., and Tiefenbacher, K. (2022). Enantioselective tail-to-head terpene cyclizations by optically active hexameric resorcin [4]arene capsule derivatives. Angew. Chem. Int. Ed. *61*, e202203384. https://doi.org/10.1002/anie.202203384.

23. Kusukawa, T., and Fujita, M. (2002). Self-assembled M_6L_4-type coordination nanocage with 2,2′-bipyridine ancillary ligands. Facile crystallization and X-ray analysis of shape-selective enclathration of neutral guests in the cage. J. Am. Chem. Soc. *124*, 13576–13582. https://doi.org/10.1021/ja020712k.

24. Pluth, M.D., and Raymond, K.N. (2007). Reversible guest exchange mechanisms in supramolecular host–guest assemblies. Chem. Soc. Rev. *36*, 161–171. https://doi.org/10.1039/B603168B.

25. Hastings, C.J., Pluth, M.D., Biros, S.M., Bergman, R.G., and Raymond, K.N. (2008). Simultaneously bound guests and chiral recognition: a chiral self-assembled supramolecular host encapsulates hydrophobic guests. Tetrahedron *64*, 8362–8367. https://doi.org/10.1016/j.tet.2008.05.131.

26. Ronson, T.K., Meng, W., and Nitschke, J.R. (2017). Design principles for the optimization of guest binding in aromatic-paneled $Fe^{II}_4L_6$ cages. J. Am. Chem. Soc. *139*, 9698–9707. https://doi.org/10.1021/jacs.7b05202.

27. Gemen, J., Church, J.R., Ruoko, T.-P., Durandin, N., Białek, M.J., Weißenfels, M., Feller, M., Kazes, M., Odaybat, M., Borin, V.A., et al. (2023). Disequilibrating azobenzenes by visible-light sensitization under confinement. Science *381*, 1357–1363. https://doi.org/10.1126/science.adh9059.

28. Caulder, D.L., Powers, R.E., Parac, T.N., and Raymond, K.N. (1998). The self-assembly of a predesigned tetrahedral M_4L_6 supramolecular cluster. Angew. Chem. Int. Ed. *37*, 1840–1843. https://doi.org/10.1002/(SICI)1521-3773(19980803)37:13/14<1840::AID-ANIE1840>3.0.CO;2-D.

29. Davis, A.V., Fiedler, D., Seeber, G., Zahl, A., Van Eldik, R., and Raymond, K.N. (2006). Guest exchange dynamics in an M_4L. J. Am. Chem. Soc. *128*, 1324–1333. https://doi.org/10.1021/ja056556+.

30. Biros, S.M., Bergman, R.G., and Raymond, K.N. (2007). The hydrophobic effect drives the recognition of hydrocarbons by an anionic metal−ligand cluster. J. Am. Chem. Soc. *129*, 12094–12095. https://doi.org/10.1021/ja075236i.

31. Morimoto, M., Cao, W., Bergman, R.G., Raymond, K.N., and Toste, F.D. (2021). Chemoselective and site-selective reductions catalyzed by a supramolecular host and a pyrdine-borane cofactor. J. Am. Chem. Soc. *143*, 2108–2114. https://doi.org/10.1021/jacs.0c12479.

32. Botteghi, C., Bianchi, M., Matteoli, U., and Benedetti, E. (1975). Asymmetric synthesis by chiral ruthenium complexes part 1, enantioselective hydrogenation of ketones and ketoximes catalysed by $H_4Ru_4(CO)_8((-)\text{-diop})_2$. Chem. Informationsdienst *6*. https://doi.org/10.1002/chin.197537127.

33. Krasik, P., and Alper, H. (1992). The ruthenium catalyzed asymmetric hydrogenation of oximes using binap as the chiral ligand. Tetrahedron Asymmetry *3*, 1283–1288. https://doi.org/10.1016/S0957-4166(00)82086-8.

34. Chan, A.S.C., Chen, C.-C., Lin, C.-W., Lin, Y.-C., Cheng, M.-C., and Peng, S.-M. (1995). The remarkable effect of E/Z isomers on the catalytic asymmetric hydrogenation of oximes. J. Chem. Soc. Chem. Commun. *1995*, 1767–1768. https://doi.org/10.1039/c39950001767.

35. Xie, Y., Mi, A., Jiang, Y., and Liu, H. (2001). Enantioselective hydrogenation of ketone oxime catalyzed by Ir-DPAMPP complex. Synth. Commun. *31*, 2767–2771. https://doi.org/10.1081/SCC-100105323.

36. Huang, K., Li, S., Chang, M., and Zhang, X. (2013). Rhodium-catalyzed enantioselective hydrogenation of oxime acetates. Org. Lett. *15*, 484–487. https://doi.org/10.1021/ol303282u.

37. Maj, A.M., Suisse, I., and Agbossou-Niedercorn, F. (2016). Asymmetric hydrogenation of 2,3-dihydro-1H-inden-1-one oxime and derivatives. Tetrahedron Asymmetry *27*, 268–273. https://doi.org/10.1016/j.tetasy.2016.02.005.

38. Rappoport, Z., and Liebman, J.F. (2009). The Chemistry of Hydroxylamines, Oximes, and Hydroxamic Acids (Wiley).

39. Mas-Roselló, J., Smejkal, T., and Cramer, N. (2020). Iridium-catalyzed acid-assisted asymmetric hydrogenation of oximes to hydroxylamines. Science *368*, 1098–1102. https://doi.org/10.1126/science.abb2559.

40. Wang, F., Chen, Y., Yu, P., Chen, G.-Q., and Zhang, X. (2022). Asymmetric hydrogenation of oximes synergistically assisted by Lewis and Brønsted acids. J. Am. Chem. Soc. *144*, 17763–17768. https://doi.org/10.1021/jacs.2c07506.

41. Li, B., Chen, J., Liu, D., Gridnev, I.D., and Zhang, W. (2022). Nickel-catalysed asymmetric hydrogenation of oximes. Nat. Chem. *14*, 920–927. https://doi.org/10.1038/s41557-022-00971-8.

42. Chang, Z.Y., and Coates, R.M. (1990). Diastereoselectivity of organometallic additions to nitrones bearing stereogenic N-substituents. J. Org. Chem. *55*, 3464–3474. https://doi.org/10.1021/jo00298a018.

43. Xia, Y., Wang, S., Miao, R., Liao, J., Ouyang, L., and Luo, R. (2022). Synthesis of *N*-alkoxy amines and hydroxylamines *via* the iridium-catalyzed transfer hydrogenation of oximes. Org. Biomol. Chem. *20*, 6394–6399. https://doi.org/10.1039/D2OB01084D.

44. Burés, J. (2016). A simple graphical method to determine the order in catalyst. Angew. Chem. Int. Ed. *55*, 2028–2031. https://doi.org/10.1002/anie.201508983.

45. Simmons, E.M., and Hartwig, J.F. (2012). On the interpretation of deuterium kinetic isotope effects in C-H bond functionalizations by transition-metal complexes. Angew. Chem. Int. Ed. *51*, 3066–3072. https://doi.org/10.1002/anie.201107334.

46. Fiedler, D., Bergman, R.G., and Raymond, K.N. (2004). Supramolecular catalysis of a unimolecular transformation: aza-Cope rearrangement within a self-assembled host. Angew. Chem. *116*, 6916–6919. https://doi.org/10.1002/ange.200461776.

47. Brown, C.J., Bergman, R.G., and Raymond, K.N. (2009). Enantioselective catalysis of the aza-Cope rearrangement by a chiral supramolecular assembly. J. Am. Chem. Soc. *131*, 17530–17531. https://doi.org/10.1021/ja906386w.

48. Bierschenk, S.M., Bergman, R.G., Raymond, K.N., and Toste, F.D. (2020). A nanovessel-catalyzed three-component aza-Darzens reaction. J. Am. Chem. Soc. *142*, 733–737. https://doi.org/10.1021/jacs.9b13177.

49. Orlandi, M., Coelho, J.A.S., Hilton, M.J., Toste, F.D., and Sigman, M.S. (2017). Parametrization of non-covalent interactions for transition state interrogation applied to asymmetric catalysis. J. Am. Chem. Soc. *139*, 6803–6806. https://doi.org/10.1021/jacs.7b02311.